Epilepsy kinase CDKL5 is a DNA damage sensor which controls transcriptional activity at DNA breaks

Taran Khanam[1,8], Ivan Muñoz[1,8], Florian Weiland[1,4], Thomas Carroll[1], Barbara N Borsos[5], Vasiliki Pantazi[5], Meghan Slean[1,6], Miroslav Novak[1,7], Rachel Toth[2], Paul Appleton[3], Tibor Pankotai[5], Houjiang Zhou[1] and John Rouse[1,9]

[1]MRC Protein Phosphorylation and Ubiquitylation Unit; and [2]MRC Reagents and Services; [3]Dundee Imaging Facility, School of Life Sciences, University of Dundee, Dundee DD1 5EH, Scotland, UK

[4]Current address: Department of Microbial and Molecular Systems (M²S), Laboratory of Enzyme, Fermentation and Brewing Technology (EFBT), Technology Campus Ghent, KU Leuven, Gebroeders De Smetstraat 1, 9000 Ghent, Belgium

[5]Department of Oral Biology and Experimental Dental Research, Faculty of Dentistry, Tisza Lajos korut 83, University of Szeged, 6722 Szeged, Hungary

[6]Current address Department of Medical Genetics, Polwarth Building, Foresterhill, Aberdeen AB25 2ZD, Scotland, UK

[7]Jacqui Wood Cancer Centre, Ninewells Hospital, University of Dundee, Dundee DD1 1UB, Scotland, UK

[8]These authors contributed equally to this work

[9]Corresponding author. Tel: +44–1382–385490; e–mail: j.rouse@dundee.ac.uk

Mutation of the *CDKL5* kinase gene leads to the seizure-prone neurodevelopmental condition CDD (CDKL5 deficiency disorder) and is the most common genetic cause of childhood epilepsy. However, the phospho-targets and roles of CDKL5 are poorly understood, especially in the nucleus. We reveal CDKL5 as a sensor of DNA damage in actively transcribed regions of the nucleus, which phosphorylates transcriptional regulators such as Elongin A (ELOA) on a specific consensus motif. Recruitment of CDKL5 and ELOA to DNA damage sites, and subsequent ELOA phosphorylation, requires both active transcription and synthesis of poly–ADP ribose to which CDKL5 can bind. Critically, CDKL5 is essential for transcriptional control at DNA breaks. Therefore, CDKL5 is a DNA damage-sensing regulator of transcription, with implications for CDKL5-related human diseases.

One sentence summary

CDKL5 kinase phosphorylates transcriptional regulators and modulates the activity of damaged transcriptional units

The protein kinases ATM, DNA-PK and ATR sense and transduce DNA damage signals, triggering a pleiotropic series of protective reactions collectively known as the DNA damage response (DDR) which prevents genome instability and disease (*1*). With the aim of expanding the repertoire of DDR kinases, we set out to find other kinases that can sense DNA damage. U–2–OS cells stably expressing mCherry–FAN1 which marks DNA damage sites, were transfected with GFP–tagged kinases individually, starting with the CMGC branch of the human kinome (Fig. S1A). BrdU–sensitized cells were laser micro-irradiated to induce a pleiotropic range of DNA lesions along a track in the nucleus. This approach revealed CDKL5 as a DNA damage sensing kinase (Fig. 1A, S1A). *CDKL5* mutations are one of the most common genetic causes of epilepsy in children (*2*), and they can lead to the severe, seizure prone neurodevelopmental disorder CDD (*3*), as well as milder syndromes (*4*). In the cytosol, CDKL5 phosphorylates microtubule regulators (*5, 6*), but the nuclear roles and targets of CDKL5 remain elusive. This prompted us to investigate how CDKL5 recognizes DNA damage, to find its nuclear targets and explore roles in DDR.

CDKL5 recruitment to sites of micro–irradiation was rapid and transient (Figs. 1A–D, Movies S1, S2), reminiscent of proteins that bind poly–ADP ribose (PAR) generated by DNA damage–activated poly–ADP ribose polymerases (PARPs) (*7*). Accordingly, CDKL5 recruitment was blocked by PARP inhibitors olaparib and talazoparib (Figs. 1B–D) or by *PARP1* disruption (Fig. S1B), but prolonged by PDD00017273, an inhibitor of PARG (poly–ADP ribose glycohydrolase) which

delays PAR degradation (Fig. 1B–D; Movies S1, S2) (*8*). CDKL5 was also retained on damaged chromatin after exposure to H_2O_2, an inducer of DNA breaks (Figs. 1E, F; S1C). Retention was prevented by olaparib, whereas nucleolar retention seen in undamaged cells was unaffected (Figs. 1E, F). Together, these data indicate that CDKL5 recruitment to DNA breaks requires synthesis of PAR, presumably by direct PAR binding although no PAR-binding motifs were detected bioinformatically. However, a series of N-terminal and C-terminal deletion constructs revealed a region between amino acids 530 and 730 necessary for CDKL5 recruitment (Figs. S2A, B), and the region 530–680 of CDKL5 was sufficient for recruitment (Figs. S2C, D). As shown in Figs. S2D–F, recombinant CDKL5 fragments corresponding to this region bound to PAR *in vitro* (Fig. S2E, F), strongly suggesting that CDKL5 senses DNA breaks by binding PAR. Accordingly, PAR was detected in CDKL5 precipitates, and vice versa, after exposure of cells to H_2O_2 (Figs. S2G,H).

These data show that PAR formation is required for CDKL5 recruitment, but we discovered unexpectedly that it is not sufficient. We found that the transcription inhibitors actinomycin D or α–amanitin which inhibit RNA polymerases (RNAPs) I and II, or DRB which blocks elongating RNAP II, abrogated the recruitment of CDKL5 to micro-irradiation sites. PAR synthesis and recruitment of the PAR-binding protein XRCC1 or FAN1 was unaffected (Figs 1G,H; S3A–D). Moreover, incubation of permeabilized cells with RNaseA abolished micro-irradiation tracks

formed by CDKL5, but not XRCC1 or FAN1 (Fig. 1I). Therefore, CDKL5 is recruited to DNA breaks at sites of active transcription.

The data above suggested that nuclear targets of CDKL5 may be involved in transcriptional control. To identify nuclear CDKL5 targets specifically, we expressed CDKL5 wild–type (WT) or a $K^{42}R$ kinase–dead (KD) mutant (*5*) exclusively in the nucleus of *CKDL5*-disrupted U–2–OS cells by adding an artificial nuclear localization signal (NLS) (Fig. S4A–C). We next compared the phosphoproteome of the two cell populations, after exposure to H_2O_2 to induce CDKL5 retention at DNA breaks (Fig. 2A, S4D, Table S1). As well as CDKL5 itself and MAP1S and EB2 (known cytosolic substrates), screening revealed a range of proteins bearing phospho–sites that were higher in abundance in $CDKL5^{NLS}$–WT cells compared with $CDKL5^{NLS}$–KD cells (>1.5–fold, $p<0.05$) (Figs. 2B, C; Table S1). Strikingly, the phospho–acceptor [S/T] residue in almost all of the putative nuclear CDKL5 substrates lies in sequence R–P–X–[**S/T**]–[A/G/P/S] (Fig. 2C), which represents a prerequisite consensus motif for CDKL5 target phosphorylation, in agreement with previous work (*5, 6*). Gene ontology (GO) analysis showed a striking enrichment of transcription regulators (Figs. 2D, E) including EP400, a chromatin-remodeling transcriptional activator (*9*), and TTDN1, mutated in a form of tricothiodystrophy (TTD), typically caused by failure in transcription–coupled DNA repair (*10*). Elongin A (ELOA), a transcriptional elongation factor and component of an E3 ligase complex which ubiquitylates RNAPII, was a top hit (*11*).

Extracted ion chromatogram (XIC) analysis of phospho–peptides isolated from FLAG-tagged EP400 (pSer^{729}), ELOA (pSer^{311}) and TTDN1 (pSer^{40}) confirmed CDKL5-dependent phosphorylation of these proteins in cells (Fig. S5A-C). Furthermore, CDKL5 robustly phosphorylated synthetic peptides corresponding to EP400 Ser^{729} and ELOA Ser^{311} demonstrating direct phosphorylation (Fig. S5D). To further investigate ELOA phosphorylation, we generated antibodies specific for phospho-Ser^{311}. Co-expression with WT, but not KD, CDKL5 markedly increased Ser^{311} phosphorylation of FLAG-ELOA, but not an ELOA Ser^{311}Ala mutant (Fig. 3A). Strikingly, CDD–associated CDKL5 mutations, which are located predominantly in the kinase catalytic domain (*12*), severely reduced CDKL5 activity towards ELOA pSer^{311}, whereas a series of benign variants did not (Fig. 3B).

CDKL5-dependent phosphorylation of endogenous ELOA Ser^{311} was evident at sites of DNA damage. Signal intensity was reduced by depletion of ELOA (Fig. 3C) or by incubation of cells with lambda-phosphatase or the ELOA Ser^{311} phosphopeptide antigen (Fig. S6A), thereby confirming antibody specificity. ELOA phosphorylation was reduced by disruption or depletion of *CDKL5* (Figs. 3D, E), or by olaparib or DRB which block CDKL5 recruitment (Fig. 3D). We wondered if ELOA is recruited to DNA damage sites by a similar mechanism to the ELOA kinase. In agreement with this idea ELOA recruitment to micro-irradiation tracks was rapid, transient, and inhibited by olaparib, α-amanitin and DRB (Fig. S6B–D). Similar results were obtained for other nuclear CDKL5

substrates such as ZNF592 and ZAP3 (Fig. S6B-D) but not EP400 (data not shown). These data reveal CDKL5-dependent phosphorylation of substrates such as ELOA at DNA damage sites, involving a common mechanism of recruitment of both kinase and substrate.

The ontological enrichment for transcription regulators among the nuclear CDKL5 substrates suggested a role in transcriptional control at DNA damage sites. Breaks in genomic DNA silence adjacent genes (*13-15*), and we tested a role for CDKL5, first using a reporter system in which a cluster of FokI nuclease–mediated DSB, induced upstream of a doxycycline inducible reporter gene, silences the reporter cassette (Fig. S7A) (*13*). Depletion of CDKL5 weakens silencing of the reporter cassette, similar to depletion of ATM or ZMYND8 (Fig. 4A; Figs. S7A–C) (*13, 14*). Second, we took advantage of a system where inducible overexpression of the site-specific meganuclease I-PpoI that cuts 14–30 times in the human genome, results in silencing of genes that sustain DSBs within or nearby. As shown in Fig. 4B, CDKL5 depletion largely abolished the I–PpoI–induced silencing of *SLCO5a1* and *RYR2* genes reported previously (*15*).

Our study reveals that CDKL5 senses DNA breaks at sites of ongoing transcription, through binding to PAR, and switches off transcription nearby (Fig. 4C). How transcriptional activity at DSB is sensed by CDKL5 remains to be investigated. Once bound to damaged DNA, CDKL5 phosphorylates transcriptional regulators including ELOA, and facilitates the silencing of genes

harboring DNA breaks; it is likely that phosphorylation of multiple CDKL5 substrates participates in silencing. For example, CDKL5 phosphorylation of ELOA could influence transcriptional elongation rates, but this remains to be ascertained. CDKL5 was recently linked to transcriptional control in a different context when it was reported to promote renal injury in mice exposed to toxic insults through up-regulating SOX9-dependent genes (*16*). We are interested in the possibility that CDKL5 controls transcription even in the absence of toxic insult, perhaps by sensing the transient DSBs induced by topoisomerases which are known to regulate transcription and impact on brain function (*17*). This will be interesting to investigate, especially as it could be particularly relevant to the pathogenesis of epilepsy and CDD.

Figure Legends

Figure 1. CDKL5 senses DNA damage in actively transcribed regions

A. BrdU–sensitized U–2–OS Flp–In T–REx stably expressing mCherry-FAN1 and GFP–NLS or GFP–CDKL5 (no NLS) were line micro-irradiated and imaged after 2min. **B.** Same as A. except that cells stably expressing GFP–NLS–CDKL5 were pre–incubated with DMSO (mock), olaparib (5 μM), talazoparib (50 nM) or PDD00017273 (0.3 μM) for 1 h prior to micro–irradiation. One of three independent experiments is shown. **C.** Same as B. except that cells were spot micro–irradiated (405 nm). **D.** Quantitation of spot intensity in C. Data represent the mean ± SEM of two independent experiments; > 50 micro–irradiated cells per point. **E.** Cells subjected to the workflow in Fig. S1C were detergent–extracted and fixed before staining with anti–GFP or fibrillarin (nucleoli). **F.** Quantification of the detergent–insoluble GFP–NLS–CDKL5 signal (minus nucleolar signal). The mean ± SD from three biological experiments is shown. Statistical significance was assessed by one-way-ANOVA-test. Asterisks ** indicate *P*–value of <0.01; ns – not significant. **G, H.** Effect of transcription inhibitors on CDKL5 recruitment after spot micro-irradiation. **I.** Stable cell lines were permeabilized and incubated with RNase A or PBS before irradiation and imaging.

Figure 2 CDKL5 phosphorylates transcriptional regulators including ELOA

A. Quantitative phosphoproteomics workflow. **B.** “Sprinkler” plot of the mass spectrometry data from the experiment in A (see Table S1). **C.** List of proteins

containing phosphorylation sites more abundant in cells expressing CDKL5^{NLS}–WT versus KD (fold change > 1.5; p-site probabilities > 0.6). **D.** Protein–protein interaction network of putative CDKL5 substrates from Table S1. Confidence levels are based on the STRING database v11.0 combined score with following bins: 150–400: low confidence (blue), 400–700: medium confidence (gold), 700–900: high confidence (not encountered in this dataset), >900: very high confidence (black). P–value was calculated as 0.00068. **E.** Analysis of GO terms. Significance cut–off was set as α = 0.01 with at least 2 proteins identified in the respective group.

Fig. 3. Phosphorylation of ELOA Ser^{311} on damaged chromatin by CDKL5

A. HEK293 cells were co-transfected with CDKL5 (wild type "WT" or kinase-dead "KD" K^{42}R mutant) fused to an NLS, and FLAG-ELOA (wild type "WT" or a S^{311}A mutant "SA"). Anti-FLAG precipitates or cell extracts were probed with the antibodies indicated. One of three independent experiments is shown. **B.** Same as A. showing a range of pathogenic (red) and benign (blue) CDKL5 variants. **C–E**. Wild type (WT), CDKL5–disrupted (CDKL5$^{\Delta/\Delta}$) or siRNA–transfected cells were subjected to indirect immunofluorescence analysis with the indicated antibodies at laser tracks. Quantification of ELOA-pSer^{311} signal at the laser tracks is shown. Data represent mean ± SD. Statistical significance was assessed by one-way-ANOVA-test. Asterisks **** indicate *P*–values of <0.0001.

Fig. 4. CDKL5 facilitates transcriptional silencing at DNA breaks

A. U–2–OS cells (263 IFII; Fig. S7A) were transfected with the siRNAs indicated. After addition of doxycycline, transcription was monitored in cells ± induction of FokI by quantification of YFP(–MS2) foci (*left*). 150 cells were analysed per condition per experiment. The mean ± SD from four independent experiments is shown. (*Right*) Quantitative RT–PCR analysis of YFP-MS2 mRNA. Data represent mean ± SD. **B**. Quantitative PCR with reverse transcription (qRT-PCR) analysis of *SLCO5a1* and *RYR2* expression levels (left) and cutting efficiencies (right) in U–2–OS HA-ER-I-PpoI cells depleted of CDKL5, at the times indicated after inducing I–PpoI. The mean ± SD from qPCR replicates of three independent experiments is shown Statistical significance for all the data was assessed by two-way-ANOVA-test **p<0.01, ***p<0.001 and ****p<0.0001; ns – not significant. **C.** Schematic diagram: CDKL5 functions in nucleus and cytosol.

Acknowledgements

We thank the technical support of the MRC-PPU including the DNA Sequencing Service, Tissue Culture team, Reagents and Services team, and the PPU Mass-Spectrometry team. We also thank Fiona Brown and James Hastie for ELOA antibody production and purification. We're grateful to Jessica Downs and Roger Greenberg for the U–2–OS cells harbouring the FokI silencing reporter, to Evi Soutoglou for U–2–OS HA-ER-I-PpoI cells, and to Nick Lakin for *PARP*-disrupted

U–2–OS cells. We’re grateful to Graeme Ball for help with microscopy data analysis. We thank Luis Sanchez-Pulido and Chris Ponting for help with bioinformatic analyses. We are grateful to members of the Rouse lab for useful discussions. This work was supported by the Medical Research Council (grant number MC_UU_12016/1; TK, IM, JR) and the pharmaceutical companies supporting the Division of Signal Transduction Therapy Unit (Boehringer-Ingelheim, GlaxoSmithKline, and Merck KGaA).

References

1. A. N. Blackford, S. P. Jackson, ATM, ATR, and DNA-PK: The Trinity at the Heart of the DNA Damage Response. *Mol Cell* **66**, 801-817 (2017).
2. J. D. Symonds *et al.*, Incidence and phenotypes of childhood-onset genetic epilepsies: a prospective population-based national cohort. *Brain* **142**, 2303-2318 (2019).
3. S. Fehr *et al.*, The CDKL5 disorder is an independent clinical entity associated with early-onset encephalopathy. *Eur J Hum Genet* **21**, 266-273 (2013).
4. C. I. MacKay *et al.*, Expanding the phenotype of the CDKL5 deficiency disorder: Are seizures mandatory? *Am J Med Genet A*, (2020).
5. I. M. Munoz *et al.*, Phosphoproteomic screening identifies physiological substrates of the CDKL5 kinase. *EMBO J* **37**, (2018).
6. L. L. Baltussen *et al.*, Chemical genetic identification of CDKL5 substrates reveals its role in neuronal microtubule dynamics. *EMBO J* **37**, (2018).
7. T. Eisemann, J. M. Pascal, Poly(ADP-ribose) polymerase enzymes and the maintenance of genome integrity. *Cell Mol Life Sci* **77**, 19-33 (2020).
8. D. I. James *et al.*, First-in-Class Chemical Probes against Poly(ADP-ribose) Glycohydrolase (PARG) Inhibit DNA Repair with Differential Pharmacology to Olaparib. *ACS Chem Biol* **11**, 3179-3190 (2016).
9. S. K. Pradhan *et al.*, EP400 Deposits H3.3 into Promoters and Enhancers during Gene Activation. *Mol Cell* **61**, 27-38 (2016).

10. E. R. Heller *et al.*, Mutations in the TTDN1 gene are associated with a distinct trichothiodystrophy phenotype. *J Invest Dermatol* **135**, 734-741 (2015).

11. R. C. Conaway, J. W. Conaway, The hunt for RNA polymerase II elongation factors: a historical perspective. *Nat Struct Mol Biol* **26**, 771-776 (2019).

12. R. Krishnaraj, G. Ho, J. Christodoulou, RettBASE: Rett syndrome database update. *Hum Mutat* **38**, 922-931 (2017).

13. N. M. Shanbhag, I. U. Rafalska-Metcalf, C. Balane-Bolivar, S. M. Janicki, R. A. Greenberg, ATM-dependent chromatin changes silence transcription in cis to DNA double-strand breaks. *Cell* **141**, 970-981 (2010).

14. F. Gong *et al.*, Screen identifies bromodomain protein ZMYND8 in chromatin recognition of transcription-associated DNA damage that promotes homologous recombination. *Genes Dev* **29**, 197-211 (2015).

15. T. Pankotai, C. Bonhomme, D. Chen, E. Soutoglou, DNAPKcs-dependent arrest of RNA polymerase II transcription in the presence of DNA breaks. *Nat Struct Mol Biol* **19**, 276-282 (2012).

16. J. Y. Kim *et al.*, A kinome-wide screen identifies a CDKL5-SOX9 regulatory axis in epithelial cell death and kidney injury. *Nat Commun* **11**, 1924 (2020).

17. P. J. McKinnon, Topoisomerases and the regulation of neural function. *Nat Rev Neurosci* **17**, 673-679 (2016).

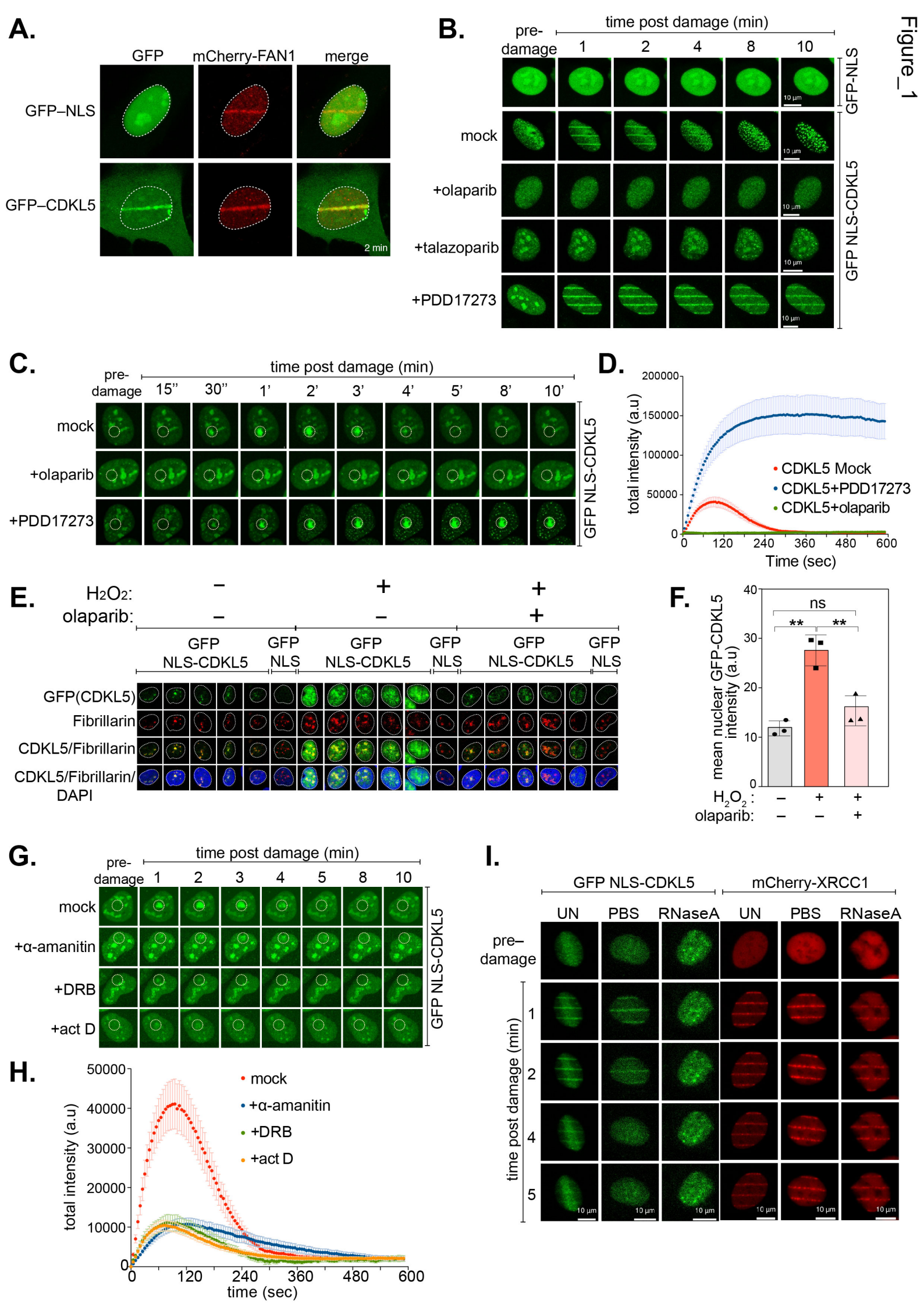
A.
GFP
mCherry-FAN1
merge
GFP–NLS
GFP–CDKL5
2 min
B.
time post damage (min)
pre-damage
1
2
4
8
10
GFP-NLS
mock
+olaparib
+talazoparib
+PDD17273
GFP NLS-CDKL5
10 µm
C.
time post damage (min)
pre-damage
15''
30''
1'
2'
3'
4'
5'
8'
10'
mock
+olaparib
+PDD17273
GFP NLS-CDKL5
D.
total intensity (a.u)
200000
150000
100000
50000
0
CDKL5 Mock
CDKL5+PDD17273
CDKL5+olaparib
0
120
240
360
480
600
Time (sec)
E.
H2O2:
olaparib:
GFP NLS-CDKL5
GFP NLS
GFP(CDKL5)
Fibrillarin
CDKL5/Fibrillarin
CDKL5/Fibrillarin/ DAPI
F.
mean nuclear GFP-CDKL5 intensity (a.u)
40
30
20
10
0
ns
**
**
H2O2 :
olaparib:
G.
time post damage (min)
pre-damage
1
2
3
4
5
8
10
mock
+α-amanitin
+DRB
+act D
GFP NLS-CDKL5
H.
total intensity (a.u)
50000
40000
30000
20000
10000
0
mock
+α-amanitin
+DRB
+act D
0
120
240
360
480
600
time (sec)
I.
GFP NLS-CDKL5
mCherry-XRCC1
UN
PBS
RNaseA
pre–damage
time post damage (min)
1
2
4
5
10 µm

Figure_2

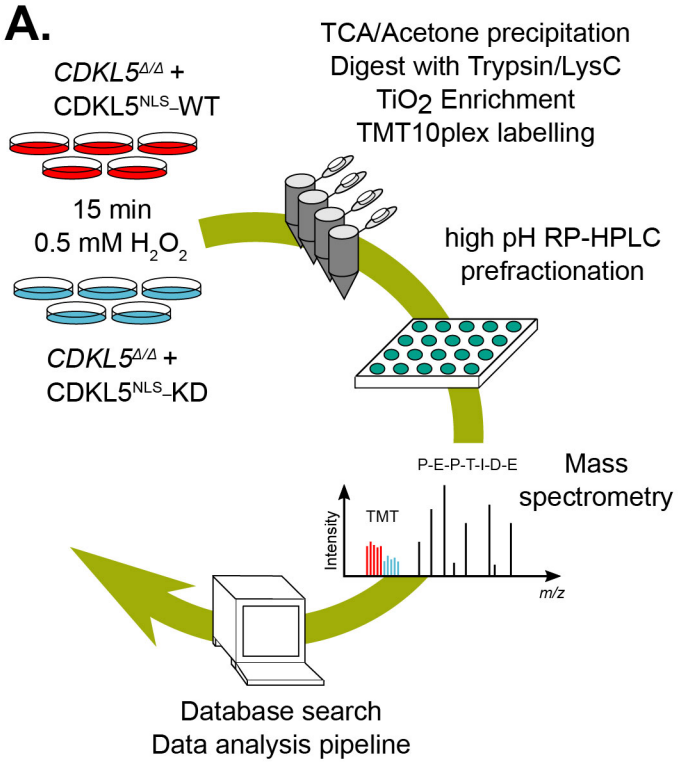

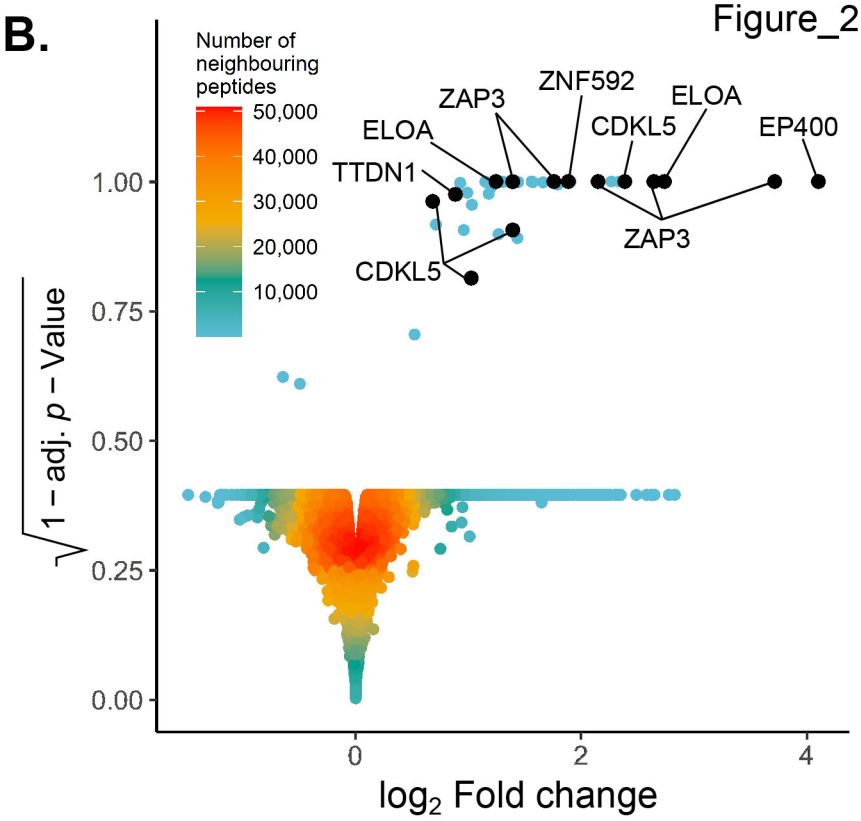

C.

Protein		Uniprot Accession Number	Fold Change	Phosphorylation Sites	Motif
EP400	E1A-binding protein p400	Q96L91	17.12	Ser729	RPSSA
ELOA	Elongin-A	Q14241	6.65	Ser311	RPPSG
ZAP3	Nuclear protein ZAP 3	P49750	6.23	Ser1089	RPGSS
CDKL5	Cyclin-dependent kinase-like 5	O76039	5.22	Tyr171	TEY
EB2	Microtubule-associated protein RP/EB family member 2	Q15555	4.8	Ser223	RPSSA
ZAP3	Nuclear protein ZAP 3	P49750	4.42	Ser1088	RPGSS
ZNF592	Zinc finger protein 592	Q92610	3.69	Ser1100	RPVSG
MAP1S	Microtubule-associated protein 1S	Q66K74	3.47	Ser900	RPLSA
SMTN	Smoothelin	P53814	3.44	Ser139	RPNSG
POM121C	Nuclear envelope pore membrane protein POM 121C	A8CG34	3.16	Ser80	RPLSS
CLSPN	Claspin	Q9HAW4	2.95	Ser1246	RPGSA
HNRNPF	Heterogeneous nuclear ribonucleoprotein F	P52597	2.7	Thr215	RPGTA
ZC3H14	Zinc finger CCCH domain-containing protein 14	Q6PJT7	2.58	Thr734	RPQTS
PHF23	PHD finger protein 23	Q9BUL5	2.47	Ser400	PKSGE
PPP1R26	Protein phosphatase 1 regulatory subunit 26	Q5T8A7	2.41	Thr606	RPSTP
RPL13	60S ribosomal protein L13	P26373	2.29	Ser52	RPASG
TNRC18	Trinucleotide repeat-containing gene 18 protein	O15417	2.26	Ser660	RPESA
ZKSCAN8	Zinc finger protein with KRAB and SCAN domains 8	Q15776	2.22	Ser141	RPVSA
QSER1	Glutamine and serine-rich protein 1	Q2KHR3	1.98	Ser1227, Ser1228	HLSSFSS
NCOA5	Nuclear receptor coactivator 5	Q9HCD5	1.94	Ser529	RPVSS
TCOF1	Treacle protein	Q13428	1.9	Ser801	APSAK
TTDN1	Tricothiodystrophy non-photosensitive 1 protein	Q8TAP9	1.84	Ser40	RPPSP
KIAA1429	Protein virilizer homolog	Q69YN4	1.64	Ser1759	RPLSS
CDKL5	Cyclin-dependent kinase-like 5	O76039	1.6	Ser847	HLSSASN

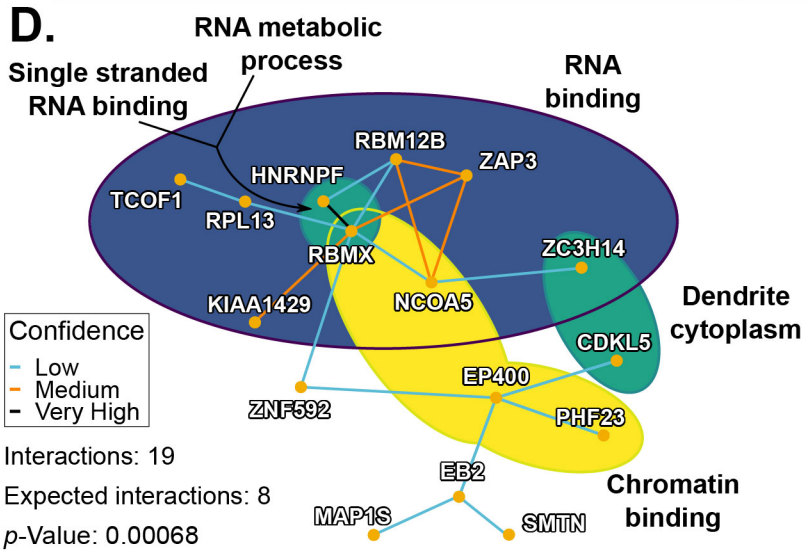

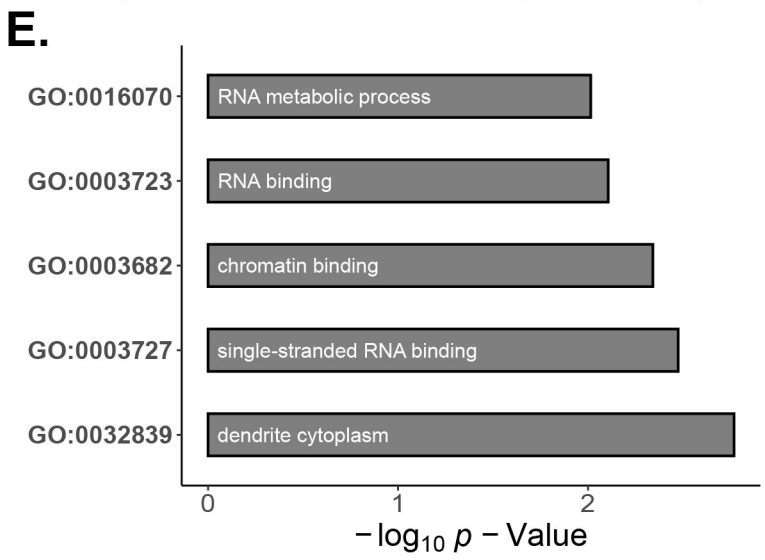

Figure_3

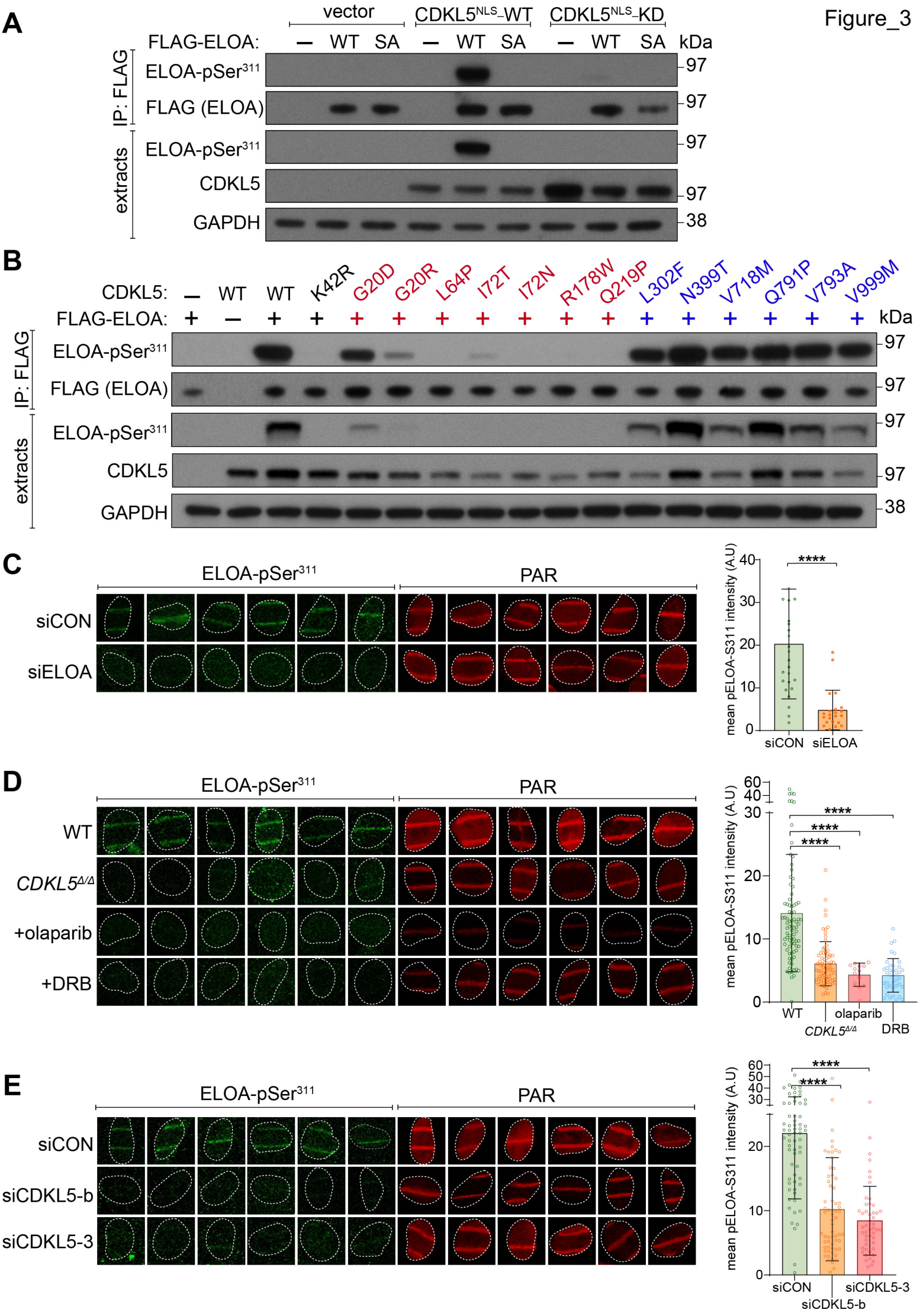
A
vector
CDKL5NLS-WT
CDKL5NLS-KD
FLAG-ELOA:
— WT SA — WT SA — WT SA
kDa
IP: FLAG
ELOA-pSer311
FLAG (ELOA)
extracts
ELOA-pSer311
CDKL5
GAPDH
97
97
97
97
38
B
CDKL5:
— WT WT K42R G20D G20R L64P I72T I72N R178W Q219P L302F N399T V718M Q791P V793A V999M
FLAG-ELOA:
+ — + + + + + + + + + + + + + + +
kDa
IP: FLAG
ELOA-pSer311
FLAG (ELOA)
extracts
ELOA-pSer311
CDKL5
GAPDH
97
97
97
97
38
C
ELOA-pSer311
PAR
siCON
siELOA
mean pELOA-S311 intensity (A.U)
40
30
20
10
0
****
siCON
siELOA
D
ELOA-pSer311
PAR
WT
CDKL5Δ/Δ
+olaparib
+DRB
mean pELOA-S311 intensity (A.U)
60
40
30
20
10
0
****
****
****
WT
CDKL5Δ/Δ
olaparib
DRB
E
ELOA-pSer311
PAR
siCON
siCDKL5-b
siCDKL5-3
mean pELOA-S311 intensity (A.U)
60
50
40
30
20
10
0
****
****
siCON
siCDKL5-b
siCDKL5-3

Figure_4

A.

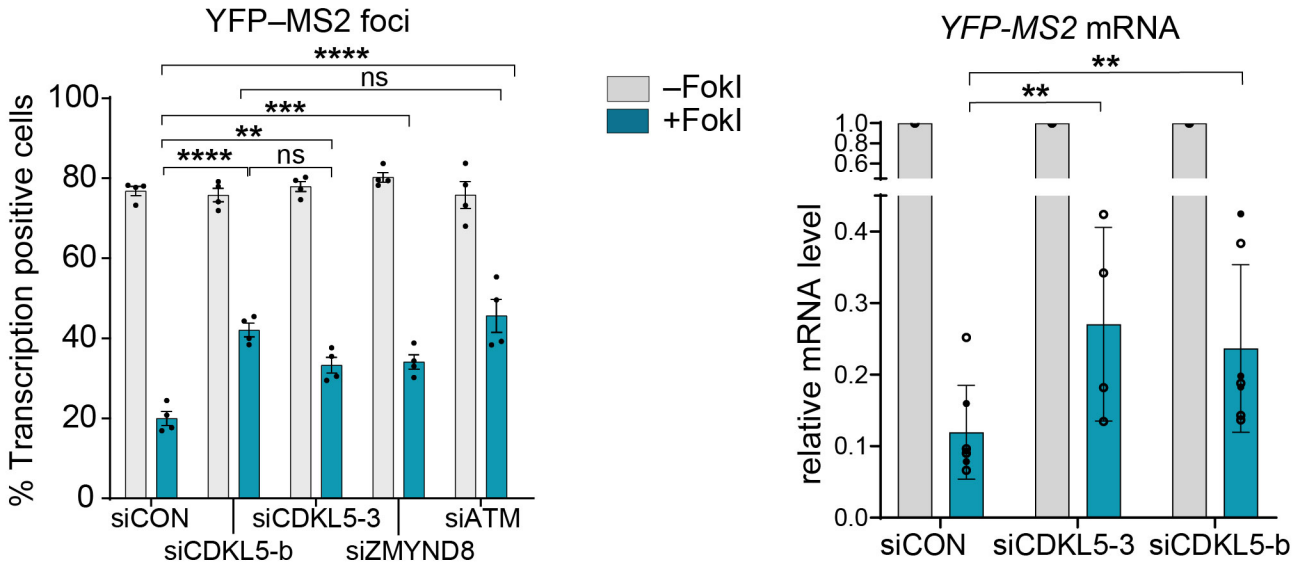
YFP–MS2 foci
% Transcription positive cells
100
80
60
40
20
0
****
ns
***
**
****
ns
–FokI
+FokI
siCON
siCDKL5-3
siATM
siCDKL5-b
siZMYND8
YFP-MS2 mRNA
relative mRNA level
1.0
0.8
0.6
0.4
0.3
0.2
0.1
0.0
**
**
siCON
siCDKL5-3
siCDKL5-b

B.

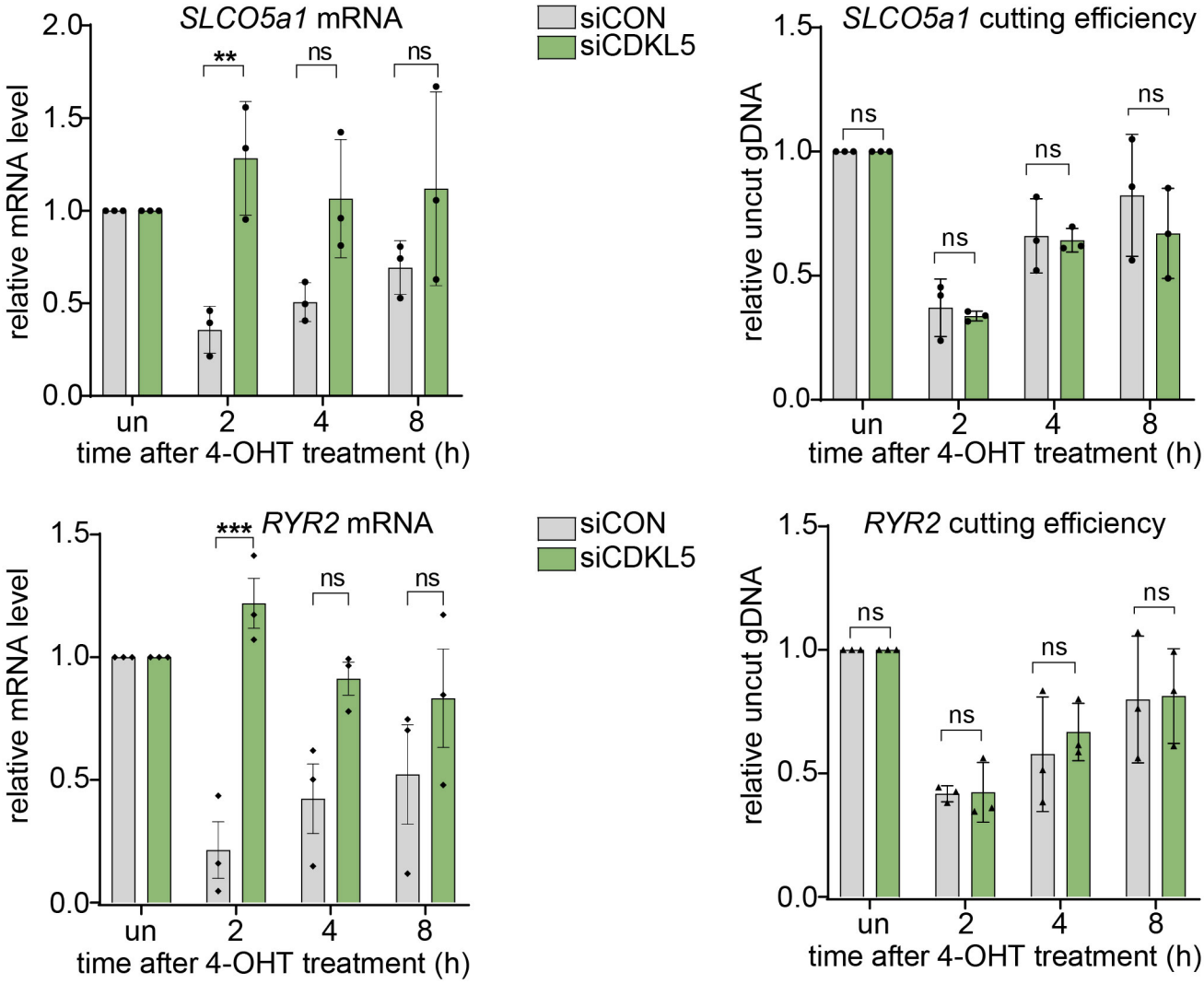
SLCO5a1 mRNA
relative mRNA level
2.0
1.5
1.0
0.5
0.0
**
ns
ns
un
2
4
8
time after 4-OHT treatment (h)
siCON
siCDKL5
SLCO5a1 cutting efficiency
relative uncut gDNA
1.5
1.0
0.5
0.0
ns
ns
ns
ns
un
2
4
8
time after 4-OHT treatment (h)
RYR2 mRNA
relative mRNA level
1.5
1.0
0.5
0.0
***
ns
ns
un
2
4
8
time after 4-OHT treatment (h)
siCON
siCDKL5
RYR2 cutting efficiency
relative uncut gDNA
1.5
1.0
0.5
0.0
ns
ns
ns
ns
un
2
4
8
time after 4-OHT treatment (h)

C.

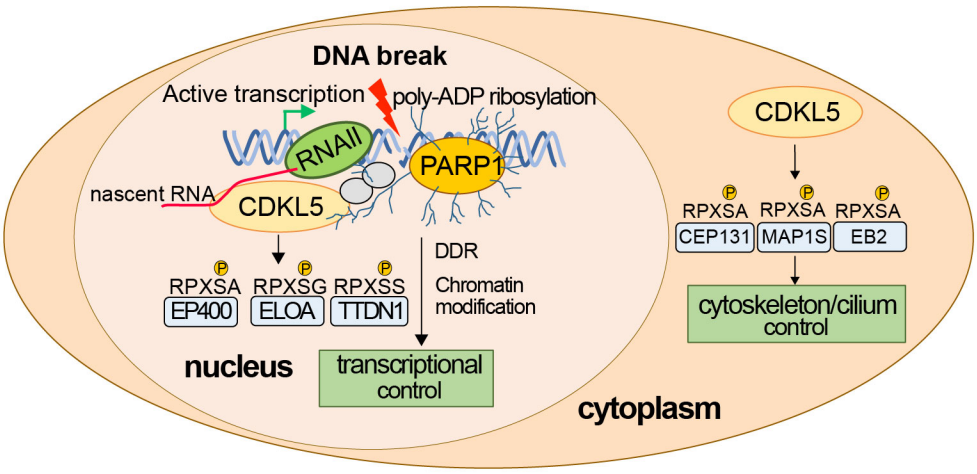
DNA break
Active transcription
poly-ADP ribosylation
RNAII
PARP1
nascent RNA
CDKL5
RPXSA
RPXSG
RPXSS
EP400
ELOA
TTDN1
DDR
Chromatin modification
nucleus
transcriptional control
CDKL5
RPXSA
RPXSA
RPXSA
CEP131
MAP1S
EB2
cytoskeleton/cilium control
cytoplasm